CANCER GENOMICS & PROTEOMICS *20*: 363-374 (2023)
doi:10.21873/cgp.20388

# Genetic Pathways in Peritoneal Mesothelioma Tumorigenesis

IOANNIS PANAGOPOULOS[1], KRISTIN ANDERSEN[1], MARTA BRUNETTI[1], LUDMILA GORUNOVA[1], BEN DAVIDSON[2,3], MARIUS LUND-IVERSEN[2], FRANCESCA MICCI[1] and SVERRE HEIM[1,3]

[1]*Section for Cancer Cytogenetics, Institute for Cancer Genetics and Informatics, The Norwegian Radium Hospital, Oslo University Hospital, Oslo, Norway;*
[2]*Department of Pathology, Oslo University Hospital, Oslo, Norway;*
[3]*Institute of Clinical Medicine, Faculty of Medicine, University of Oslo, Oslo, Norway*

**Abstract.** *Background/Aim: Mesotheliomas are tumors similar to, and probably derived from, mesothelial cells. They carry acquired chromosomal rearrangements, deletions affecting CDKN2A, pathogenetic polymorphisms in NF2, and fusion genes which often contain the promiscuous EWSR1, FUS, and ALK as partner genes. Here, we report the cytogenomic results on two peritoneal mesotheliomas. Materials and Methods: Both tumors were examined using G-banding with karyotyping and array comparative genomic hybridization (aCGH). One of them was further investigated with RNA sequencing, reverse transcription polymerase chain reaction (RT-PCR), Sanger sequencing, and fluorescence in situ hybridization (FISH). Results: In the first mesothelioma, the karyotype was 25~26,X,+5,+7,+20[cp4]/50~52,idemx2[cp7]/46,XX[2]. aCGH detected gains of chromosomes 5, 7, and 20 with retained heterozygosity on these chromosomes. In the second tumor, the karyotype was 46,XX,inv(10)(p11q25)[7]/46,XX[3]. aCGH did not detect any gains or losses and showed heterozygosity for all chromosomes. RNA sequencing, RT-PCR/Sanger sequencing, and FISH showed that the inv(10) fused MAP3K8 from 10p11 with ABLIM1 from 10q25. The MAP3K8::ABLIM1 chimera lacked exon 9 of MAP3K8. Conclusion: Our data, together with information on previously described mesotheliomas, illustrate two pathogenetic mechanisms in peritoneal mesothelioma: One pathway is characterized by hyperhaploidy, but with retained disomies for chromosomes 5, 7, and 20; this may be particularly prevalent in biphasic mesotheliomas. The second pathway is characterized by rearrangements of MAP3K8 from which exon 9 of MAP3K8 is lost. The absence of exon 9 from oncogenetically rearranged MAP3K8 is a common theme in thyroid carcinoma, lung cancer, and spitzoid as well as other melanoma subtypes.*

*Correspondence to:* Ioannis Panagopoulos, Section for Cancer Cytogenetics, Institute for Cancer Genetics and Informatics, The Norwegian Radium Hospital, Oslo University Hospital, Montebello, PO Box 4954 Nydalen, NO-0424 Oslo, Norway. Tel: +47 22782362, email: ioannis.panagopoulos@rr-research.no

*Key Words:* Peritoneal mesothelioma, biphasic mesothelioma, hyperhaploidy, disomic chromosomes, inv(10)(p11q25), *MAP3K8::ABLIM1* chimeric gene, exon 9 of *MAP3K8*.



Mesotheliomas are rare, mostly malignant tumors similar to, and probably derived from, mesothelial cells, *i.e.*, the cells lining the body's serous cavities (1-3). More than 80% of mesotheliomas are developed in the wall lining of the pleural cavity, 7% in the peritoneum, 1% in the pericardium, and less than 1% in the tunica vaginalis (4, 5). The three histological types, epithelioid, sarcomatoid, and biphasic (the latter subtype has both epithelioid and sarcomatous differentiation), account for 50-60%, 10%, and 30-40% of mesotheliomas, respectively (3), and influence disease prognosis (6, 7). Malignant mesothelioma is strongly associated with exposure to asbestos (8-11). Other etiological factors are genetic predisposition (12-14), radiation exposure, and viral infection that alone or together with asbestos exposure can cause malignant mesotheliomas (15, 16).

Mesotheliomas carry acquired genetic aberrations (17). Cytogenetic analysis of 131 tumors has shown that most mesotheliomas have complex karyotypes (18). Comparative genomic hybridization, loss of heterozygosity, and fluorescence in situ hybridization (FISH) studies have detected nonrandom gains and losses of chromosomal regions (19-21). Deletions of or from chromosome arms 1p, 3p, 6q, 9p, 15q, and 22q are frequent, homozygous deletions have been found to be the main mechanism affecting p16/CDKN2A (on 9p21), and inactivating mutations coupled with allelic loss were found to involve the *NF2* locus (on 22q12) (17, 22).

Next generation sequencing (also called high throughput sequencing, deep sequencing *etcetera*) techniques were

shown to be a valuable tool in detecting acquired genetic alterations in mesothelioma (23-26) and RNA sequencing was found to be a powerful tool for detection of fusion genes in cancer (27, 28). Using sequential combination of karyotyping and RNA-sequencing (27), our group detected an *EWSR1::YY1* chimera and its reciprocal *YY1::EWSR1* fusion transcript in a malignant mesothelioma carrying a t(14;22)(q32;q12) chromosomal translocation (29). In the same study, we identified another malignant mesothelioma carrying an *EWSR1::YY1* fusion gene and concluded that a subgroup of malignant mesotheliomas is indeed characterized by *EWSR1::YY1* (29). Two years later and using the same sequential methodology, we found novel *TNS3::MAP3K3* and *ZFPM2::ELF5* fusion genes in a multicystic mesothelioma with t(7;17)(p12;q23) and t(8;11)(q23;p13) (30). Our early findings and conclusions were later confirmed by other investigators (31-37). The reported fusion genes often contain the promiscuous *EWSR1* and *FUS* as 5′-end partners (33, 37) and the likewise promiscuous *ALK* as the 3′-partner gene (34, 35). In addition, some of the fusion genes found in mesotheliomas are also present in the neoplastic cells of other tumors. For example, the *EWSR1::ATF1* and *FUS::ATF1* fusion genes are found in clear cell sarcomas and angiomatoid fibrous histiocytomas (38-42) whereas *EWSR1::NR4A3* is found in extraskeletal myxoid chondrosarcoma (43-45). Here, we report our genetic findings on two additional peritoneal mesotheliomas with characteristic genetic profiles.

## Materials and Methods

*Ethics statement*. The study was approved by the Regional Committee for Medical and Health Research Ethics, South-East Norway (S-07474a, REK Sør-Øst). Written informed consent was obtained from patients prior to publication of the case details. The Ethics Committee's approval included a review of the consent procedure. All patient information has been de-identified.

*Case 1*. A 42-year-old woman underwent right-sided ileocolectomy after examination of a preoperative needle biopsy had revealed a clear cell, vascular, tumor-suspect lesion. An abdominal tumor measuring 10×9×6 cm was found. Microscopic evaluation revealed a highly cellular tumor, in some areas with dilated vascular spaces (Figure 1A). In some parts, it was made up of spindle cells with overt atypia forming vessel-like spaces (Figure 1B). Vascular formations lined by less atypical cells were seen in other areas (Figure 1C) and in other still, epithelioid cells with a clear cytoplasm and low-grade atypia predominated (Figure 1D). Immunohistochemistry (IHC) showed expression of pan-cytokeratin (AE1/AE3) and partial expression of CK5/6, calretinin (Figure 1E), and podoplanin (D2-40) in the epithelioid areas. KIT (CD117), EMA, WT1, PECAM1 (CD31), SMA, desmin, ERG, CD34, DOG1, PAX8, SALL4, SF1, PMEL (HMB45), MLANA (melan A), TNFRSF8 (CD30), synaptophysin, CLDN4 (claudin-4), and STAT6 were negative. BAP1 was retained. The differential diagnosis was between mesothelioma and hemangiopericytoma. The tumor was sent for consultation to Massachusetts General Hospital (Boston, MA, USA) where the diagnosis of biphasic mesothelioma was favored.

*Case 2*. A 25-year-old woman was diagnosed with a papillary well-differential benign mesothelial tumor based on examination of a preoperative needle biopsy. She subsequently underwent left-sided salpingo-oophorectomy, omentectomy, appendectomy, and excision of various peritoneal lesions. A papillary tumor measuring 9×5×4 cm was found on the surface of the left ovary. Microscopic examination of the ovarian tumor showed cells with characteristic mesothelial morphology, predominantly in areas of papillary growth (Figure 2A and B) but also in foci with solid growth (Figure 2C), forcing a modification of the diagnosis to malignant mesothelioma. Tumor tissue was additionally found in two preoperative peritoneal biopsies. IHC of them showed expression of calretinin (Figure 2D), WT1 (Figure 2E), and podoplanin (D2-40) (Figure 2F) but loss of desmin confirming the malignant diagnosis. EMA staining was negative. BAP1 was retained.

*G-banding and karyotyping*. Samples from the surgically removed tumors were short-term cultured as described elsewhere (46, 47). In brief, a part of resected specimens was minced with scalpels into 1-2 mm fragments and enzymatically disaggregated with collagenase II (Worthington, Freehold, NJ, USA). The resulting cells were cultured, harvested, and processed for cytogenetic examination (46, 47). Chromosome preparations were G-banded with Wright's stain (Sigma Aldrich, St Louis, MO, USA) and examined. Metaphases were analyzed and karyograms prepared using the CytoVision computer-assisted karyotyping system (Leica Biosystems, Newcastle upon Tyne, UK). The karyotypes were described according to the International System for Human Cytogenomic Nomenclature (48).

*Genomic DNA extraction and array comparative genomic hybridization (aCGH) analysis*. aCGH was performed using the CytoSure array products (Oxford Gene Technology, Begbroke, Oxfordshire, UK) following the company's protocols (49). The array combines long-oligo probes for copy number variant (CNV) detection alongside single nucleotide polymorphism (SNP) probes for identification of loss-of-heterozygosity (LOH). Genomic DNA was extracted using the Maxwell RSC instrument System and the Maxwell RSC Tissue DNA Kit (Promega, Madison, WI, USA) and the concentration was measured with a Quantus fluorometer (Promega). The reference DNA was Promega's human genomic DNA (Promega). The slides (CytoSure Cancer +SNP array) were scanned in an Agilent SureScan Dx microarray scanner using Agilent Feature Extraction Software (version 12.1.1.1). Data were analyzed using the CytoSure Interpret analysis software (version 4.9.40). Apart from copy number variation (CNV), the software detects allelic imbalance and loss-of-heterozygosity based on the B-allele frequency methodology (50). The software annotations are based on human genome build 19.

*Total RNA extraction and RNA sequencing*. Total RNA was extracted using the miRNeasy Mini Kit (Qiagen, Hilden, Germany) and the QiaCube automated purification system (Qiagen) and the concentration was measured with the QIAxpert microfluidic UV/VIS spectrophotometer (Qiagen). One μg of total RNA was sent to the Genomics Core Facility (http://genomics.no/oslo/) at the Norwegian Radium Hospital, Oslo University Hospital for high-throughput paired-end RNA-sequencing. The software FusionCatcher was used to detect possible fusion transcripts (51, 52).

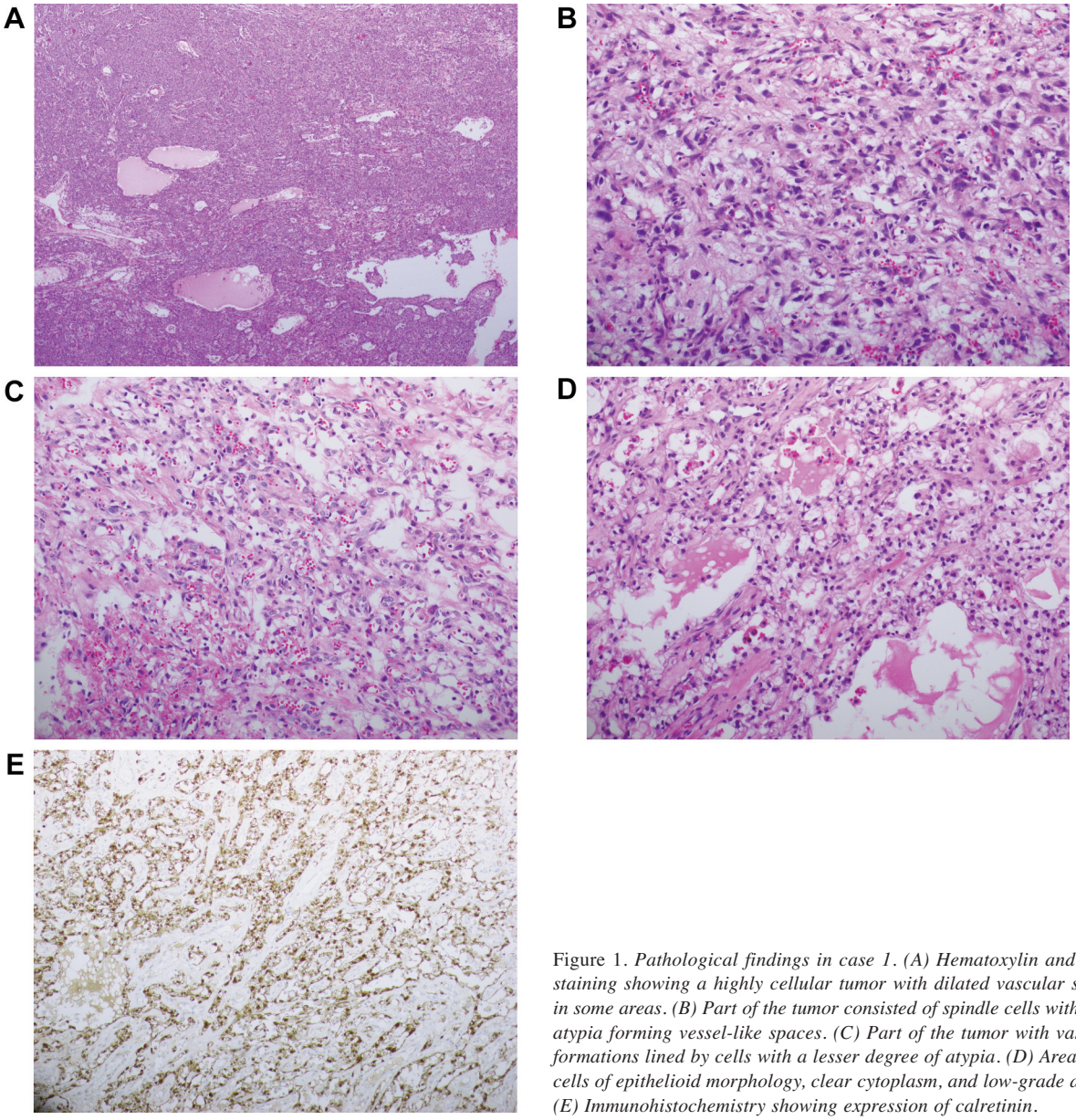


Figure 1. *Pathological findings in case 1. (A) Hematoxylin and eosin staining showing a highly cellular tumor with dilated vascular spaces in some areas. (B) Part of the tumor consisted of spindle cells with overt atypia forming vessel-like spaces. (C) Part of the tumor with vascular formations lined by cells with a lesser degree of atypia. (D) Areas with cells of epithelioid morphology, clear cytoplasm, and low-grade atypia. (E) Immunohistochemistry showing expression of calretinin.*

*Reverse transcription polymerase chain reaction (RT-PCR) and Sanger sequencing analyses*. cDNA was synthesized from one μg of total RNA using the iScript Advanced cDNA Synthesis Kit for RT-qPCR according to the manufacturer's instructions (Bio-Rad, Hercules, CA, USA). cDNA corresponding to 20 ng total RNA was used as template in subsequent PCR assays. The quality of the cDNA synthesis was assessed by amplification of a cDNA fragment of the ABL protooncogene 1, non-receptor tyrosine kinase (*ABL1*) gene using the primer combination ABL1-91F1/ABL1-404R1 (53). In order to confirm the existence of the chimeric fusion, RT-PCR and Sanger sequencing analyses were performed using the Direct Cycle Sequencing Kit according to the company's recommendations (ThermoFisher Scientific, Waltham, MA, USA). The primers were M13For-MAP3K8-1577F1: TGTAAAACGACGGCCAGT CCC AAG AGC CGC AGA CCT ACT AA and M13Rev-ABLIM1-407R1: CAGGAAACA GCTATGACC GAA ATG TTT GGT CTG GAC CCG AA.

Sequencing was run on the Applied Biosystems SeqStudio Genetic Analyzer system (ThermoFisher Scientific). The Basic Local Alignment Search Tool (BLAST) was used to compare the sequences obtained by Sanger sequencing with the NCBI reference sequences NM_005204.4 of the mitogen-activated protein kinase 8 (*MAP3K8*), transcript variant 1, and NM_002313.7 of actin binding LIM protein 1 (*ABLIM1*), transcript variant 1 (54). The BLAST-like alignment tool (BLAT) and the human genome browser at UCSC were also used to map the sequences on the Human GRCh37/hg19 assembly (55, 56).

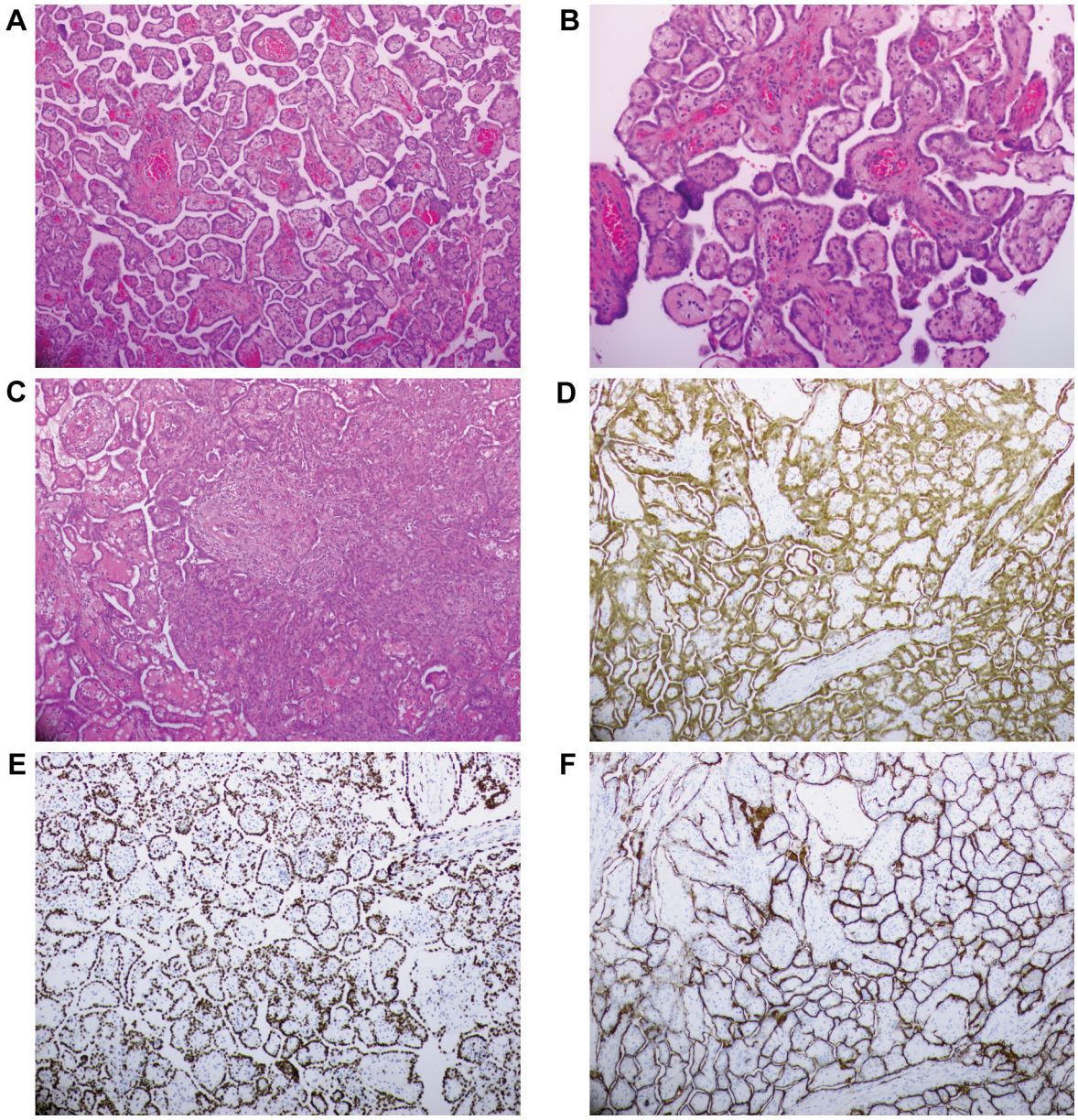


Figure 2. *Pathological findings in case 2. (A) Hematoxylin and eosin staining showing cells with characteristic mesothelial morphology, predominantly in areas of papillary growth. (B) Higher magnification of the area shown in A. (C) Cells with characteristic mesothelial morphology in foci with solid growth. (D) Immunohistochemistry showing expression of calretinin. (E) Immunohistochemistry showing expression of WT1. (F) Immunohistochemistry showing expression of D2-40.*

*Fluorescence in situ hybridization (FISH).* FISH analysis was performed using in-house prepared probes as previously described (57, 58). The probes were made from commercially available bacterial artificial chromosomes (BAC) purchased from the BACPAC Resource Center operated by BACPAC Genomics (Emeryville, CA, USA). BAC clones retrieved from the RPCI-11 Human BAC library were selected according to physical and genetic mapping data on p and q arms of chromosome 10 (see below) as reported on the Human Genome Browser at the University of California, Santa Cruz browser on Human GRCH38/hg38 (56). In addition, FISH mapping of the clones on normal controls was performed to confirm their chromosomal location. The probe for the *MAP3K8* gene was BAC RP11-350D11 (accession numbers AQ530804.1, AQ530801.1, AZ516988.1, and AZ516986.1) mapping to 10p11.23 at position chr10:30346217-30536207. The probe for the *ABLIM1* gene was composed from

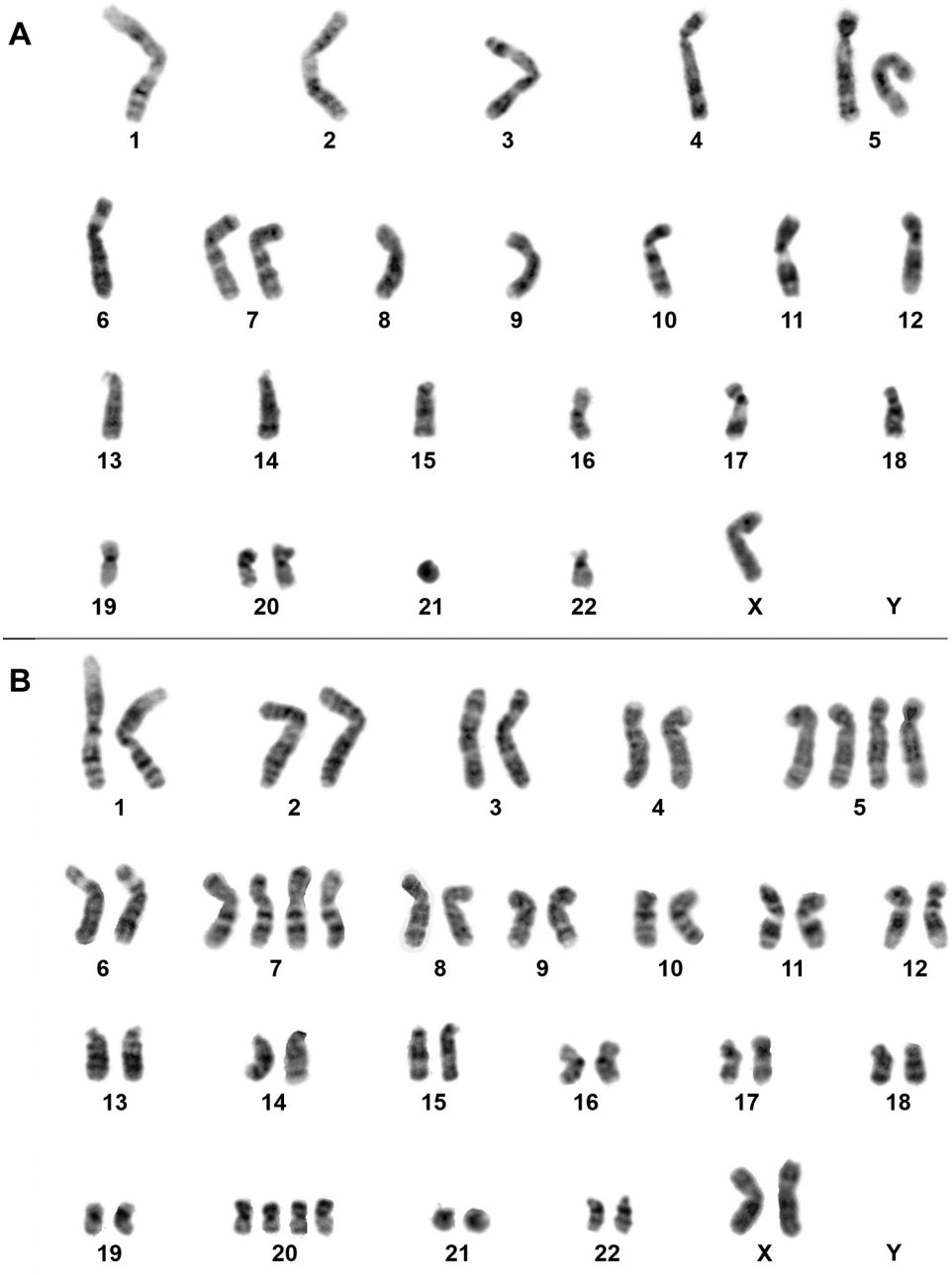


Figure 3. *Cytogenetic analysis of case 1. (A) Karyogram from the hyperhaploid clone with karyotype 26,X,+5,+7,+20. (B) Karyogram showing a duplicated clone with the karyotype 52,XX,+5,+5,+7,+7,+20,+20.*

BAC clones RP11-317F20 (accession numbers AQ535184.1, AQ535181.1, and AL133384.12) and RP11-620D7 (accession numbers AQ404856 and AQ401659) mapping to 10q25.3 at positions chr10:114366439-114534062 and chr10:114698913-114887429, respectively. DNA was extracted and probes were labelled and hybridized as previously described (57, 58). The probe for the *MAP3K8* gene was labelled with Texas Red-5-dUTP (PerkinElmer, Boston, MA, USA) to obtain a red signal whereas the probe for the *ABLIM1* gene was labelled with fluorescein-12-dUTP (PerkinElmer) to obtain a green signal. Chromosome preparations were counterstained with 0.2 μg/ml DAPI and overlaid with a 24×50 $mm^2$ coverslip. Fluorescent signals were captured and analyzed using the CytoVision system (Applied Imaging, Newcastle, UK).

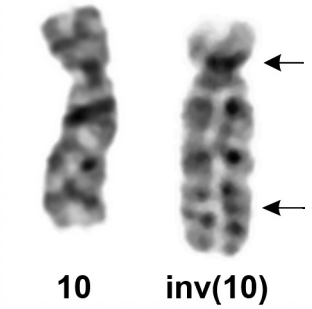


Figure 4. *Cytogenetic analysis of case 2. Partial karyogram showing pericentric inv(10)(p11q25) together with the normal chromosome 10. Arrows indicate breakpoints.*

## Results

Both mesotheliomas had clonal chromosomal abnormalities in their neoplastic cells. Two karyotypically related clones were found in the first mesothelioma: one hyperhaploid with 25~26 chromosomes without any structural aberrations (Figure 3A) and its duplicated version, a hyperdiploid clone with 50~52 chromosomes (Figure 3B). The karyotype was 25~26,X,+5,+7,+20[cp4]/50~52,idemx2[cp7]/46,XX[2] (Figure 3). A single pericentric inversion involving bands 10p11 and 10q25 was found in seven out of 10 metaphase spreads from the second peritoneal mesothelioma corresponding to the karyotype 46,XX,inv(10)(p11q25)[7]/46,XX[3] (Figure 4).

In the mesothelioma with hyperhaploidy aCGH detected gains of chromosomes 5, 7, and 20 (data not shown) with retained heterozygosity on these chromosomes (Table I). In the second peritoneal mesothelioma with inv(10)(p11q25), aCGH did not detect any gains or losses (data not shown) and showed heterozygosity for all chromosomes (Table I).

Analysis of the RNA sequencing data using the FusionCatcher software detected three *MAP3K8::ABLIM1* and one *ABLIM1::MAP3K8* chimeric transcript in the only tumor examined using these techniques, the mesothelioma with inv(10)(p11q25) (Table II).

RT-PCR/cycle (Sanger) sequencing verified the presence of the *MAP3K8::ABLIM1* chimeric transcript in which exon 8 of *MAP3K8* (nt 1722 of sequence with accession number NM_005204.4) fused to exon 2 of *ABLIM1* (nt 320 of sequence with accession number NM_002313.7) (Figure 5A). No other chimeric transcripts were examined by RT-PCR/cycle (Sanger) sequencing.

FISH analysis on metaphase spreads using in-house prepared *MAP3K8* and *ABLIM1* probes on chromosome bands 10p11 and 10q25, respectively (Figure 5B), showed fusion (yellow) signals on both the p and q arm of the inv(10)(p11q25) chromosome whereas a red (*MAP3K8*) and a green (*ABLIM1*) signal were seen on the normal chromosome 10 (Figure 5C).

## Discussion

Near-haploid karyotypes are rare, reported in less than 1% of cytogenetically investigated neoplastic lesions (18, 59). They may occur in both hematological malignancies and solid tumors (18, 59-63). In the mesothelioma context, a near-haploid karyotype was first reported in a biphasic peritoneal mesothelioma (63), and subsequent studies have shown that biphasic mesotheliomas are indeed genetically characterized by genomic near-haploidization (64-66). Chromosomes 5 and 7 always remain disomic in these karyotypes and half of the reported cases also have two copies of chromosome 20 (63-66). Thus, the karyotype of the present biphasic mesothelioma - 25~26,X,+5,+7,+20[cp4]/55~56,idemx2[cp7]/46,XX[2] - is in full agreement with the previously established picture of biphasic mesothelioma karyotypes (63-66).

Disomy for chromosomes 5, 7, and 20 has also been reported to be a feature of hyperhaploid chondrosarcomas (59) and inflammatory leiomyosarcomas (67). Using B allele frequency methodology (50) on the hyperhaploid tumor of the present study, we found that the disomic chromosomes 5, 7, and 20 retained heterozygosity. This agrees with previous observations that in tumors with near-haploid karyotypes, the disomic chromosomes are maternal and paternal (67-69). Hyperhaploidy may affect thousands of genes and may result in massive loss of heterozygosity. In inflammatory leiomyosarcoma, which is cytogenetically characterized by hyperhaploidy, disomic chromosomes were found to have higher gene expression levels than monosomic chromosomes (67). The mechanisms whereby hyperhaploidy contributes to tumorigenesis, are unknown, however, although disturbed gene dosage balance may play a role in the development of biphasic mesothelioma as well as other hyperhaploid tumor types (70, 71).

The *MAP3K8* gene has nine exons (NCBI reference sequence: NM_005204.4) and codes for a cytoplasmic protein that is a member of the serine/threonine protein kinase family and activates both the MAP and JNK kinase pathways (72-74). Truncations of *MAP3K8* were found in thyroid carcinoma (75, 76) and lung cancer (77) whereas both truncations and fusion genes of *MAP3K8* were found in spitzoid melanomas (78) and other melanoma subtypes (79-82). In all tumors with *MAP3K8* rearrangements, lack of exon 9 was a common pathogenetic theme (76). Exon 9 of *MAP3K8* codes for the last 43 amino acids of the MAP3K8 protein (position 425-467 in reference sequence NP_005195.2: DSSCTGSTEESEMLKRQRSLY IDLGALAGYFNLVRGPPTLEYG). This part of the protein is a kinase repression domain, has a degradation signal (degron) between positions 435 and 457 (SEMLKRQRSLYIDLGA LAGYFNL), and a portion of the PEST sequence (DSSCTG STEESEML) which acts as a signal for MAP3K8 degradation (83). Absence of the last 43 amino acids results in stabilization of the truncated MAP3K8 protein, higher kinase activity, and

Table I. *Homozygosity observed for each chromosome in the hyperhaploid mesothelioma (case 1) and the mesothelioma carrying inv(10)(p11q25) (case 2).*

| Chr: Number of SNP probes | Peritoneal mesothelioma, case 1 | | Peritoneal mesothelioma, case 2 | |
|---|---|---|---|---|
| | HH/HE/UG | Homozygosity (%) | HH/HE/UG | Homozygosity (%) |
| Chr 1: 1180 | 1165/12/3 | 99 | 682/490/8 | 58 |
| Chr 2: 1584 | 1572/11/1 | 99 | 981/591/12 | 62 |
| Chr 3: 1483 | 1461/19/3 | 99 | 903/575/5 | 61 |
| Chr 4: 1101 | 1076/20/5 | 98 | 646/446/9 | 59 |
| Chr 5: 1037 | 702/317/18 | 69 | 599/427/11 | 58 |
| Chr 6: 1113 | 1101/11/1 | 99 | 647/460/6 | 58 |
| Chr 7: 1145 | 763/360/22 | 68 | 661/475/9 | 58 |
| Chr 8: 1225 | 1203/20/2 | 98 | 693/521/11 | 57 |
| Chr 9: 828 | 818/9/1 | 99 | 450/368/10 | 55 |
| Chr 10: 946 | 933/9/4 | 99 | 565/376/5 | 60 |
| Chr 11: 893 | 879/12/2 | 99 | 562/324/7 | 63 |
| Chr 12: 770 | 759/9/2 | 99 | 442/320/8 | 58 |
| Chr 13: 758 | 747/8/3 | 99 | 441/308/9 | 59 |
| Chr 14: 567 | 562/5/0 | 99 | 334/225/8 | 60 |
| Chr 15: 529 | 526/3/0 | 99 | 304/224/1 | 58 |
| Chr 16: 530 | 520/10/0 | 98 | 276/248/6 | 53 |
| Chr 17: 487 | 477/7/3 | 99 | 273/212/2 | 56 |
| Chr 18: 571 | 563/7/1 | 99 | 316/249/6 | 56 |
| Chr 19: 213 | 208/4/1 | 98 | 117/94/2 | 55 |
| Chr 20: 388 | 277/108/3 | 72 | 241/145/2 | 62 |
| Chr 21: 339 | 334/5/0 | 99 | 196/140/3 | 58 |
| Chr 22: 205 | 199/4/2 | 98 | 119/85/1 | 58 |
| Chr X: 878 | 865/10/3 | 99 | 493/372/13 | 57 |

Chr: Chromosome; SNP: single nucleotide polymorphism; HH/HE/UG: homozygous genotype/heterozygous genotype/unknown genotype.

Table II. *The MAP3K8::ABLIM1 and ABLIM1::MAP3K8 fusion transcripts detected in peritoneal mesothelioma carrying inv(10)(p11q25) after analysis of RNA sequencing data with FusionCatcher. Exons are based on the reference sequences NM_005204.4 for MAP3K8 and NM_002313.7 for ABLIM1.*

| Fusion transcript | Spanning reads | Fusion_sequence |
|---|---|---|
| *MAP3K8::ABLIM1* (exon 8-exon 2)* | 27 | CTGCTGAGTAGGAAGGAGCTGGAACTTCCTGAGAACATTGCTG:<br>:TGGCCCACCCTCAGGACCCTCACCACCCATCAGAGAAGCCTGT |
| *MAP3K8::ABLIM1* (exon 8-exon 3)* | 5 | CTGCTGAGTAGGAAGGAGCTGGAACTTCCTGAGAACATTGCTG:<br>:TGTGTGGCTGTGACCTGGCACAAGGGGGCTTCTTCATAAAGAA |
| *MAP3K8::ABLIM1* (exon 8-exon 5)* | 3 | CTGCTGAGTAGGAAGGAGCTGGAACTTCCTGAGAACATTGCTG:<br>:ATTGTGCCGGCTGCGGAAGAGATATCAAGAATGGGCAGGCGCT |
| *ABLIM1::MAP3K8* (exon 8-exon 8) | 2 | TGGCATCCCGACTGTAAGCAATCTACGAAGACCGAGGAAAAGCTGCGGGT:<br>:ATGAGGCCCTGAACCCGCCCAGAGAGGATCAGCCACGCTGTCAGAGTCTG |

*In-frame fusion transcripts.

higher oncogenic capacity (83, 84). Truncated MAP3K8 protein was indeed found to have much higher transformation activity than does wild-type MAP3K8 (75-78, 85).

*ABLIM1* encodes a protein that binds to actin filaments and mediates interactions between actin and cytoplasmic targets (86). This protein, together with the proteins encoded by *ABLIM2* (on 4p16) and *ABLIM3* (on 5q32), constitute the actin-binding LIM (ABLIM) protein family (86-89). At the N-terminal end, ABLIM proteins contain four LIM zinc-binding domains, followed by an ABLIM anchor superfamily domain and a Villin headpiece domain at the C-terminal end (86-89).

In the peritoneal mesothelioma with inv(10)(p11q25), based on the reference sequences NM_005204.4/ NP_005195.2 for *MAP3K8* and NM_002313.7/ NP_002304.3 for *ABLIM1*, the *MAP3K8::ABLIM1* chimera lacks exon 9 of *MAP3K8*, a fusion gene feature similar to all previously reported *MAP3K8*

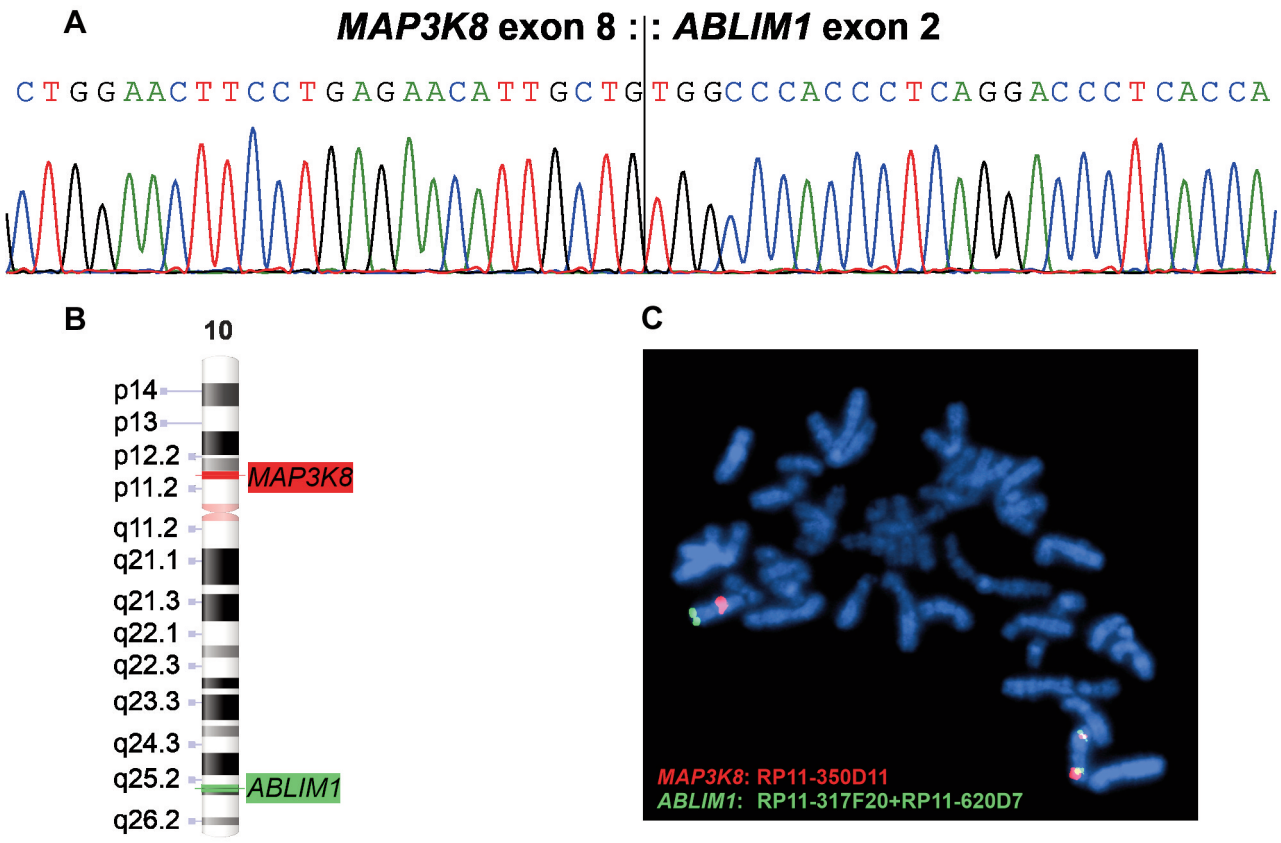


Figure 5. *Sanger sequencing and fluorescence in situ hybridization (FISH) of peritoneal mesothelioma currying inv(10)(p11q25). (A) Partial chromatogram showing the fusion point of exon 8 of MAP3K8 with exon 2 of ABLIM1. (B) Ideogram of chromosome 10 showing the position of the genes MAP3K8 and ABLIM1. (C) FISH on a metaphase spread showing yellow fusion signals on the p and q arms of inv(10)(p11q25) together with red (MAP3K8) and green (ABLIM1) signals on the normal chromosome 10.*

rearrangements (see above). The *MAP3K8::ABLIM1* is predicted to code for a 1121 amino acid long chimeric protein containing the catalytic domain of the Serine/Threonine kinase of MAP3K8 and all functional domains of ABLIM1. The exact cellular role of the chimeric protein is unknown; for that, functional studies are required.

In conclusion, we present the genetic analyses of two mesotheliomas that have developed *via* alternative pathogenetic mechanisms. The dominating feature of the first was karyotypic hyperhaploidy, but with disomies of chromosomes 5,7, and 20, a pattern that appears to be characteristic of biphasic mesotheliomas. The second displayed a *MAP3K8::ABLIM1* fusion gene from which exon 9 of *MAP3K8* was missing. This pathogenetic mechanism is described for the first time in mesothelioma but appears to be a common theme for *MAP3K8*-rearrangements in other tumor types.

## Conflicts of Interest

The Authors declare that they have no potential conflicts of interest.

## Authors' Contributions

IP designed and supervised the research, performed molecular genetic experiments, bioinformatics analyses, and wrote the manuscript. KA performed molecular genetic experiments, fluorescence *in situ* hybridization, and interpreted the data. MB performed molecular genetic experiments. LG performed the cytogenetic analysis. BD performed the pathological examination. ML-I performed the pathological examination. FM evaluated the data. SH assisted with experimental design and writing of the manuscript. All Authors read and approved of the final manuscript.

## References

1 Mutsaers S: The mesothelial cell. Int J Biochem Cell Biol 36(1): 9-16, 2004. DOI: 10.1016/s1357-2725(03)00242-5

2 Asciak R, George V, Rahman N: Update on biology and management of mesothelioma. Eur Respir Rev 30(159): 200226, 2021. DOI: 10.1183/16000617.0226-2020

3 Janes S, Alrifai D, Fennell D: Perspectives on the treatment of malignant pleural mesothelioma. N Engl J Med 385(13): 1207-1218, 2021. DOI: 10.1056/NEJMra1912719

4 Hassan R, Alexander R: Nonpleural mesotheliomas: mesothelioma of the peritoneum, tunica vaginalis, and pericardium. Hematol Oncol Clin North Am 19(6): 1067-1087, 2005. DOI: 10.1016/j.hoc.2005.09.005

5 Moore AJ, Parker RJ, Wiggins J: Malignant mesothelioma. Orphanet J Rare Dis 3: 34, 2008. DOI: 10.1186/1750-1172-3-34

6 Brcic L, Kern I: Clinical significance of histologic subtyping of malignant pleural mesothelioma. Transl Lung Cancer Res 9(3): 924-933, 2020. DOI: 10.21037/tlcr.2020.03.38

7 Mastromarino M, Lenzini A, Aprile V, Alì G, Bacchin D, Korasidis S, Ambrogi M, Lucchi M: New insights in pleural mesothelioma classification update: diagnostic traps and prognostic implications. Diagnostics 12(12): 2905, 2022. DOI: 10.3390/diagnostics12122905

8 Fonte R, Gambettino S, Melazzini M, Scelsi M, Zanon C, Candura S: Asbestos-induced peritoneal mesothelioma in a construction worker. Environ Health Perspect 112(5): 616-619, 2004. DOI: 10.1289/ehp.6542

9 Bianchi C, Bianchi T: Malignant mesothelioma: global incidence and relationship with asbestos. Ind Health 45(3): 379-387, 2007. DOI: 10.2486/indhealth.45.379

10 Candura SM, Canto A, Amatu A, Gerardini M, Stella G, Mensi M, Poggi G: Malignant mesothelioma of the tunica vaginalis testis in a petrochemical worker exposed to asbestos. Anticancer Res 28(2b): 1365-1368, 2008.

11 Mangone L, Storchi C, Pinto C, Giorgi Rossi P, Bisceglia I, Romanelli A: Incidence of malignant mesothelioma and asbestos exposure in the Emilia-Romagna region, Italy. Med Lav 113(5): e2022047, 2022. DOI: 10.23749/mdl.v113i5.13312

12 Testa J, Cheung M, Pei J, Below J, Tan Y, Sementino E, Cox N, Dogan A, Pass H, Trusa S, Hesdorffer M, Nasu M, Powers A, Rivera Z, Comertpay S, Tanji M, Gaudino G, Yang H, Carbone M: Germline BAP1 mutations predispose to malignant mesothelioma. Nat Genet 43(10): 1022-1025, 2011. DOI: 10.1038/ng.912

13 Betti M, Aspesi A, Sculco M, Matullo G, Magnani C, Dianzani I: Genetic predisposition for malignant mesothelioma: A concise review. Mutat Res Rev Mutat Res 781: 1-10, 2019. DOI: 10.1016/j.mrrev.2019.03.001

14 Panou V, Røe O: Inherited genetic mutations and polymorphisms in malignant mesothelioma: a comprehensive review. Int J Mol Sci 21(12): 4327, 2020. DOI: 10.3390/ijms21124327

15 Attanoos R, Churg A, Galateau-Salle F, Gibbs A, Roggli V: Malignant mesothelioma and its non-asbestos causes. Arch Pathol Lab Med 142(6): 753-760, 2018. DOI: 10.5858/arpa.2017-0365-RA

16 Attanoos R, Churg A, Galateau-Salle F, Gibbs A, Roggli V: In reply to "Malignant mesothelioma and its nonasbestos causes". Arch Pathol Lab Med 143(8): 911-914, 2019. DOI: 10.5858/arpa.2019-0060-LE

17 Lee WC, Testa JR: Somatic genetic alterations in human malignant mesothelioma (review). Int J Oncol 14(1): 181-188, 1999.

18 Mitelman F, Johansson B, Mertens F: Mitelman database of chromosome aberrations and gene fusions in cancer. 2023. Available at: https://mitelmandatabase.isb-cgc.org/ [Last accessed on April 27, 2023]

19 Musti M, Kettunen E, Dragonieri S, Lindholm P, Cavone D, Serio G, Knuutila S: Cytogenetic and molecular genetic changes in malignant mesothelioma. Cancer Genet Cytogenet Cytogenetics 170(1): 9-15, 2006. DOI: 10.1016/j.cancergencyto.2006.04.011

20 Taniguchi T, Karnan S, Fukui T, Yokoyama T, Tagawa H, Yokoi K, Ueda Y, Mitsudomi T, Horio Y, Hida T, Yatabe Y, Seto M, Sekido Y: Genomic profiling of malignant pleural mesothelioma with array-based comparative genomic hybridization shows frequent non-random chromosomal alteration regions including JUN amplification on 1p32. Cancer Sci 98(3): 438-446, 2007. DOI: 10.1111/j.1349-7006.2006.00386.x

21 Takeda M, Kasai T, Enomoto Y, Takano M, Morita K, Kadota E, Iizuka N, Maruyama H, Nonomura A: Genomic gains and losses in malignant mesothelioma demonstrated by FISH analysis of paraffin-embedded tissues. J Clin Pathol 65(1): 77-82, 2012. DOI: 10.1136/jclinpath-2011-200208

22 Thurneysen C, Opitz I, Kurtz S, Weder W, Stahel R, Felley-Bosco E: Functional inactivation of NF2/merlin in human mesothelioma. Lung Cancer 64(2): 140-147, 2009. DOI: 10.1016/j.lungcan.2008.08.014

23 Miyanaga A, Masuda M, Tsuta K, Kawasaki K, Nakamura Y, Sakuma T, Asamura H, Gemma A, Yamada T: Hippo pathway gene mutations in malignant mesothelioma: Revealed by RNA and targeted exon sequencing. J Thorac Oncol 10(5): 844-851, 2015. DOI: 10.1097/jto.0000000000000493

24 Kang H, Kim H, Lee S, Mendez P, Kim J, Woodard G, Yoon J, Jen K, Fang L, Jones K, Jablons D, Kim I: Whole exome and targeted deep sequencing identify genome-wide allelic loss and frequent SETDB1 mutations in malignant pleural mesotheliomas. Oncotarget 7(7): 8321-8331, 2016. DOI: 10.18632/oncotarget.7032

25 Naka T, Hatanaka Y, Marukawa K, Okada H, Hatanaka K, Sakakibara-Konishi J, Oizumi S, Hida Y, Kaga K, Mitsuhashi T, Matsuno Y: Comparative genetic analysis of a rare synchronous collision tumor composed of malignant pleural mesothelioma and primary pulmonary adenocarcinoma. Diagn Pathol 11(1): 38, 2016. DOI: 10.1186/s13000-016-0488-0

26 Ugurluer G, Chang K, Gamez ME, Arnett AL, Jayakrishnan R, Miller RC, Sio TT: Genome-based mutational analysis by next generation sequencing in patients with malignant pleural and peritoneal mesothelioma. Anticancer Res 36(5): 2331-2338, 2016.

27 Panagopoulos I, Thorsen J, Gorunova L, Micci F, Heim S: Sequential combination of karyotyping and RNA-sequencing in the search for cancer-specific fusion genes. Int J Biochem Cell Biol 53: 462-465, 2014. DOI: 10.1016/j.biocel.2014.05.018

28 Kumar S, Razzaq S, Vo A, Gautam M, Li H: Identifying fusion transcripts using next generation sequencing. WIREs RNA 7(6): 811-823, 2016. DOI: 10.1002/wrna.1382

29 Panagopoulos I, Thorsen J, Gorunova L, Micci F, Haugom L, Davidson B, Heim S: RNA sequencing identifies fusion of theEWSR1andYY1genes in mesothelioma with t(14;22)(q32;q12). Genes, Chromosomes and Cancer 52(8): 733-740, 2013. DOI: 10.1002/gcc.22068

30 Panagopoulos I, Gorunova L, Davidson B, Heim S: Novel TNS3-MAP3K3 and ZFPM2-ELF5 fusion genes identified by RNA sequencing in multicystic mesothelioma with t(7;17)(p12;q23) and t(8;11)(q23;p13). Cancer Lett 357(2): 502-509, 2015. DOI: 10.1016/j.canlet.2014.12.002

31 Desmeules P, Joubert P, Zhang L, Al-Ahmadie H, Fletcher C, Vakiani E, Delair D, Rekhtman N, Ladanyi M, Travis W, Antonescu C: A subset of malignant mesotheliomas in young adults are associated with recurrent EWSR1/FUS-ATF1 fusions. Am J Surg Pathol 41(7): 980-988, 2017. DOI: 10.1097/PAS.0000000000000864

32 Hung Y, Dong F, Watkins J, Nardi V, Bueno R, Dal Cin P, Godleski J, Crum C, Chirieac L: Identification of ALK rearrangements in malignant peritoneal mesothelioma. JAMA Oncol 4(2): 235, 2018. DOI: 10.1001/jamaoncol.2017.2918

33 Argani P, Harvey I, Nielsen G, Takano A, Suurmeijer A, Voltaggio L, Zhang L, Sung Y, Stenzinger A, Mechtersheimer G, Dickson B, Antonescu C: EWSR1/FUS-CREB fusions define a distinctive malignant epithelioid neoplasm with predilection for mesothelial-lined cavities. Mod Pathol 33(11): 2233-2243, 2020. DOI: 10.1038/s41379-020-0646-5

34 Argani P, Lian D, Agaimy A, Metzler M, Wobker S, Matoso A, Epstein J, Sung Y, Zhang L, Antonescu C: Pediatric mesothelioma with ALK fusions. Am J Surg Pathol 45(5): 653-661, 2021. DOI: 10.1097/PAS.0000000000001656

35 Miyagawa C, Takaya H, Sakai K, Nishio K, Konishi M, Minamiguchi S, Shimada T, Matsumura N: A novel malignant peritoneal mesothelioma with STRN Exon 2 and ALK exon 20: a case report and literature review. The Oncologist 26(5): 356-361, 2021. DOI: 10.1002/onco.13714

36 Agaimy A, Brcic L, Briski L, Hung Y, Michal M, Michal M, Nielsen G, Stoehr R, Rosenberg A: NR4A3 fusions characterize a distinctive peritoneal mesothelial neoplasm of uncertain biological potential with pure adenomatoid/microcystic morphology. Genes, Chromosomes Cancer 62(5): 256-266, 2023. DOI: 10.1002/gcc.23118

37 Dermawan J, Torrence D, Lee C, Villafania L, Mullaney K, Dinapoli S, Sukhadia P, Benayed R, Borsu L, Agaram N, Nash G, Dickson B, Benhamida J, Antonescu C: EWSR1:: YY1 fusion positive peritoneal epithelioid mesothelioma harbors mesothelioma epigenetic signature: Report of 3 cases in support of an emerging entity. Genes, Chromosomes Cancer 61(10): 592-602, 2022. DOI: 10.1002/gcc.23074

38 Zucman J, Delattre O, Desmaze C, Epstein A, Stenman G, Speleman F, Fletchers C, Aurias A, Thomas G: EWS and ATF-1 gene fusion induced by t(12;22) translocation in malignant melanoma of soft parts. Nat Genet 4(4): 341-345, 1993. DOI: 10.1038/ng0893-341

39 Waters B, Panagopoulos I, Allen E: Genetic characterization of angiomatoid fibrous histiocytoma identifies fusion of the FUS and ATF-1 genes induced by a chromosomal translocation involving bands 12q13 and 16p11. Cancer Genet Cytogenet 121(2): 109-116, 2000. DOI: 10.1016/s0165-4608(00)00237-5

40 Panagopoulos I, Mertens F, Dêbiec-Rychter M, Isaksson M, Limon J, Kardas I, Domanski H, Sciot R, Perek D, Crnalic S, Larsson O, Mandahl N: Molecular genetic characterization of the EWS/ATF1 fusion gene in clear cell sarcoma of tendons and aponeuroses. Int J Cancer 99(4): 560-567, 2002. DOI: 10.1002/ijc.10404

41 Raddaoui E, Donner L, Panagopoulos I: Fusion of the FUS and ATF1 genes in a large, deep-seated angiomatoid fibrous histiocytoma. Diagn Mol Pathol 11(3): 157-162, 2002. DOI: 10.1097/00019606-200209000-00006

42 Hallor K, Mertens F, Jin Y, Meis-Kindblom J, Kindblom L, Behrendtz M, Kalén A, Mandahl N, Panagopoulos I: Fusion of theEWSR1 andATF1 genes without expression of theMITF-M transcript in angiomatoid fibrous histiocytoma. Genes, Chromosomes Cancer 44(1): 97-102, 2005. DOI: 10.1002/gcc.20201

43 Labelle Y, Zucman J, Stenman G, Kindblom L, Knight J, Turc-Carel C, Dockhorn-Dworniczak B, Mandahl N, Desmaze C, Peter M, Aurias A, Delattre O, Thomas G: Oncogenic conversion of a novel orphan nuclear receptor by chromosome translocation. Hum Mol Genet 4(12): 2219-2226, 1995. DOI: 10.1093/hmg/4.12.2219

44 Clark J, Benjamin H, Gill S, Sidhar S, Goodwin G, Crew J, Gusterson BA, Shipley J, Cooper CS: Fusion of the EWS gene to CHN, a member of the steroid/thyroid receptor gene superfamily, in a human myxoid chondrosarcoma. Oncogene 12(2): 229-235, 1996.

45 Panagopoulos I, Mertens F, Isaksson M, Domanski H, Brosjö O, Heim S, Bjerkehagen B, Sciot R, Dal Cin P, Fletcher J, Fletcher C, Mandahl N: Molecular genetic characterization of the EWS/CHN and RBP56/CHN fusion genes in extraskeletal myxoid chondrosarcoma. Genes, Chromosomes Cancer 35(4): 340-352, 2002. DOI: 10.1002/gcc.10127

46 Polito P, Dal Cin P, Debiec-Rychter M, Hagemeijer A: Human solid tumors: cytogenetic techniques. Methods Mol Biol 220: 135-150, 2003. DOI: 10.1385/1-59259-363-1:135

47 Lukeis R, Suter M: Cytogenetics of solid tumours. Methods Mol Biol 730: 173-187, 2011. DOI: 10.1007/978-1-61779-074-4_13

48 McGowan-Jordan J, Hastings RJ, Moore S: ISCN 2020: An International system for human cytogenomic nomenclature. Basel, Switzerland, Karger, 2020.

49 Panagopoulos I, Gorunova L, Andersen K, Lund-Iversen M, Lobmaier I, Micci F, Heim S: NDRG1-PLAG1 and TRPS1-PLAG1 fusion genes in chondroid syringoma. Cancer Genomics Proteomics 17(3): 237-248, 2020. DOI: 10.21873/cgp.20184

50 Staaf J, Lindgren D, Vallon-Christersson J, Isaksson A, Goransson H, Juliusson G, Rosenquist R, Hoglund M, Borg A, Ringner M: Segmentation-based detection of allelic imbalance and loss-of-heterozygosity in cancer cells using whole genome SNP arrays. Genome Biol 9(9): R136, 2008. DOI: 10.1186/gb-2008-9-9-r136

51 Kangaspeska S, Hultsch S, Edgren H, Nicorici D, Murumägi A, Kallioniemi O: Reanalysis of RNA-sequencing data reveals several additional fusion genes with multiple isoforms. PLoS ONE 7(10): e48745, 2012. DOI: 10.1371/journal.pone.0048745

52 Nicorici D, Satalan M, Edgren H, Kangaspeska S, Murumagi A, Kallioniemi O, Virtanen S, Kilkku O: FusionCatcher - a tool for finding somatic fusion genes in paired-end RNA-sequencing data. bioRxiv, 2014. DOI: 10.1101/011650

53 Torkildsen S, Brunetti M, Gorunova L, Spetalen S, Beiske K, Heim S, Panagopoulos I: Rearrangement of the chromatin organizer special AT-rich binding protein 1 gene, SATB1, resulting from a t(3;5)(p24;q14) chromosomal translocation in acute myeloid leukemia. Anticancer Res 37(2): 693-698, 2017. DOI: 10.21873/anticanres.11365

54 Altschul S, Gish W, Miller W, Myers E, Lipman D: Basic local alignment search tool. J Mol Biol 215(3): 403-410, 1990. DOI: 10.1016/S0022-2836(05)80360-2

55 Kent WJ: BLAT--the BLAST-like alignment tool. Genome Res 12(4): 656-664, 2002. DOI: 10.1101/gr.229202

56 Kent W, Sugnet C, Furey T, Roskin K, Pringle T, Zahler A, Haussler a: The Human Genome Browser at UCSC. Genome Res 12(6): 996-1006, 2002. DOI: 10.1101/gr.229102

57 Panagopoulos I, Andersen K, Gorunova L, Davidson B, Micci F, Heim S: A novel cryptic t(2;3)(p21;q25) translocation fuses the WWTR1 and PRKCE genes in uterine leiomyoma with 3q- as the sole visible chromosome abnormality. Cancer Genomics Proteomics 19(5): 636-646, 2022. DOI: 10.21873/cgp.20348

58 Panagopoulos I, Gorunova L, Andersen K, Lund-Iversen M, Hognestad H, Lobmaier I, Micci F, Heim S: Chromosomal

translocation t(5;12)(p13;q14) leading to fusion of high-mobility group AT-hook 2 gene with intergenic sequences from chromosome sub-band 5p13.2 in benign myoid neoplasms of the breast: a second case. Cancer Genomics Proteomics 19(4): 445-455, 2022. DOI: 10.21873/cgp.20331

59 Mandahl N, Johansson B, Mertens F, Mitelman F: Disease-associated patterns of disomic chromosomes in hyperhaploid neoplasms. Genes, Chromosomes and Cancer 51(6): 536-544, 2012. DOI: 10.1002/gcc.21947

60 Safavi S, Paulsson K: Near-haploid and low-hypodiploid acute lymphoblastic leukemia: two distinct subtypes with consistently poor prognosis. Blood 129(4): 420-423, 2017. DOI: 10.1182/blood-2016-10-743765

61 Haas O, Borkhardt A: Hyperdiploidy: the longest known, most prevalent, and most enigmatic form of acute lymphoblastic leukemia in children. Leukemia 36(12): 2769-2783, 2022. DOI: 10.1038/s41375-022-01720-z

62 Dal Cin P, Sciot R, Fletcher C, Samson I, De Vos R, Mandahl N, Willén H, Larsson O, Van den Berghe H: Inflammatory leiomyosarcoma may be characterized by specific near-haploid chromosome changes. J Pathol 185(1): 112-115, 1998. DOI: 10.1002/(sici)1096-9896(199805)185:1<112::Aid-path54>3.0.Co;2-u

63 Sukov W, Ketterling R, Wei S, Monaghan K, Blunden P, Mazzara P, Raghavan R, Oliviera A, Wiktor A, Keeney G, Van Dyke D: Nearly identical near-haploid karyotype in a peritoneal mesothelioma and a retroperitoneal malignant peripheral nerve sheath tumor. Cancer Genet Cytogenet 202(2): 123-128, 2010. DOI: 10.1016/j.cancergencyto.2010.07.120

64 Hmeljak J, Sanchez-Vega F, Hoadley KA, Shih J, Stewart C, Heiman D, Tarpey P, Danilova L, Drill E, Gibb EA, Bowlby R, Kanchi R, Osmanbeyoglu HU, Sekido Y, Takeshita J, Newton Y, Graim K, Gupta M, Gay CM, Diao L, Gibbs DL, Thorsson V, Iype L, Kantheti H, Severson DT, Ravegnini G, Desmeules P, Jungbluth AA, Travis WD, Dacic S, Chirieac LR, Galateau-Salle F, Fujimoto J, Husain AN, Silveira HC, Rusch VW, Rintoul RC, Pass H, Kindler H, Zauderer MG, Kwiatkowski DJ, Bueno R, Tsao AS, Creaney J, Lichtenberg T, Leraas K, Bowen J, Network TR, Felau I, Zenklusen JC, Akbani R, Cherniack AD, Byers LA, Noble MS, Fletcher JA, Robertson AG, Shen R, Aburatani H, Robinson BW, Campbell P, Ladanyi M: Integrative molecular characterization of malignant pleural mesothelioma. Cancer Discov 8(12): 1548-1565, 2018. DOI: 10.1158/2159-8290.CD-18-0804

65 Hung Y, Dong F, Dubuc A, Dal Cin P, Bueno R, Chirieac L: Molecular characterization of localized pleural mesothelioma. Mod Pathol 33(2): 271-280, 2020. DOI: 10.1038/s41379-019-0330-9

66 Hung Y, Dong F, Torre M, Crum C, Bueno R, Chirieac L: Molecular characterization of diffuse malignant peritoneal mesothelioma. Mod Pathol 33(11): 2269-2279, 2020. DOI: 10.1038/s41379-020-0588-y

67 Nord K, Paulsson K, Veerla S, Wejde J, Brosjö O, Mandahl N, Mertens F: Retained heterodisomy is associated with high gene expression in hyperhaploid inflammatory leiomyosarcoma. Neoplasia 14(9): 807-IN5, 2012. DOI: 10.1593/neo.12930

68 Bovée J, Van Royen M, Bardoel A, Rosenberg C, Cornelisse C, Cleton-Jansen A, Hogendoorn P: Near-haploidy and subsequent polyploidization characterize the progression of peripheral chondrosarcoma. Am J Pathol 157(5): 1587-1595, 2000. DOI: 10.1016/s0002-9440(10)64796-7

69 Olsson L, Paulsson K, Bovée J, Nord K: Clonal evolution through loss of chromosomes and subsequent polyploidization in chondrosarcoma. PLoS ONE 6(9): e24977, 2011. DOI: 10.1371/journal.pone.0024977

70 Veitia R: Gene dosage balance in cellular pathways. Genetics 168(1): 569-574, 2004. DOI: 10.1534/genetics.104.029785

71 Veitia R, Birchler J: Dominance and gene dosage balance in health and disease: why levels matter! J Pathol 220(2): 174-185, 2010. DOI: 10.1002/path.2623

72 Vougioukalaki M, Kanellis D, Gkouskou K, Eliopoulos A: Tpl2 kinase signal transduction in inflammation and cancer. Cancer Lett 304(2): 80-89, 2011. DOI: 10.1016/j.canlet.2011.02.004

73 Xu D, Matsumoto M, McKenzie B, Zarrin A: TPL2 kinase action and control of inflammation. Pharmacol Res 129: 188-193, 2018. DOI: 10.1016/j.phrs.2017.11.031

74 Njunge L, Estania A, Guo Y, Liu W, Yang L: Tumor progression locus 2 (TPL2) in tumor-promoting inflammation, tumorigenesis and tumor immunity. Theranostics 10(18): 8343-8364, 2020. DOI: 10.7150/thno.45848

75 Miyoshi J, Higashi T, Mukai H, Ohuchi T, Kakunaga T: Structure and transforming potential of the human cot oncogene encoding a putative protein kinase. Mol Cell Biol 11(8): 4088-4096, 1991. DOI: 10.1128/mcb.11.8.4088-4096.1991

76 Panagopoulos I, Heim S: Neoplasia-associated chromosome translocations resulting in gene truncation. Cancer Genomics Proteomics 19(6): 647-672, 2022. DOI: 10.21873/cgp.20349

77 Clark A, Reynolds S, Anderson M, Wiest J: Mutational activation of theMAP3K8 protooncogene in lung cancer. Genes, Chromosomes Cancer 41(2): 99-108, 2004. DOI: 10.1002/gcc.20069

78 Newman S, Fan L, Pribnow A, Silkov A, Rice S, Lee S, Shao Y, Shaner B, Mulder H, Nakitandwe J, Shurtleff S, Azzato E, Wu G, Zhou X, Barnhill R, Easton J, Nichols K, Ellison D, Downing J, Pappo A, Potter P, Zhang J, Bahrami A: Clinical genome sequencing uncovers potentially targetable truncations and fusions of MAP3K8 in spitzoid and other melanomas. Nat Med 25(4): 597-602, 2019. DOI: 10.1038/s41591-019-0373-y

79 Lehmann B, Shaver T, Johnson D, Li Z, Gonzalez-Ericsson P, Sánchez V, Shyr Y, Sanders M, Pietenpol J: Identification of targetable recurrent MAP3K8 rearrangements in melanomas lacking known driver mutations. Mol Cancer Res 17(9): 1842-1853, 2019. DOI: 10.1158/1541-7786.MCR-19-0257

80 Quan V, Zhang B, Mohan L, Shi K, Isales M, Panah E, Taxter T, Beaubier N, White K, Gerami P: Activating structural alterations in MAPK genes are distinct genetic drivers in a unique subgroup of Spitzoid neoplasms. Am J Surg Pathol 43(4): 538-548, 2019. DOI: 10.1097/PAS.0000000000001213

81 Houlier A, Pissaloux D, Masse I, Tirode F, Karanian M, Pincus L, McCalmont T, LeBoit P, Bastian B, Yeh I, De la Fouchardière A: Melanocytic tumors with MAP3K8 fusions: report of 33 cases with morphological-genetic correlations. Mod Pathol 33(5): 846-857, 2020. DOI: 10.1038/s41379-019-0384-8

82 Quan V, Zhang B, Zhang Y, Mohan L, Shi K, Wagner A, Kruse L, Taxter T, Beaubier N, White K, Zou L, Gerami P: Integrating next-generation sequencing with morphology improves prognostic and biologic classification of Spitz neoplasms. J Invest Dermatol 140(8): 1599-1608, 2020. DOI: 10.1016/j.jid.2019.12.031

83 Gándara M, López P, Hernando R, Castaño J, Alemany S: The COOH-terminal domain of wild-type cot regulates its stability and kinase specific activity. Mol Cell Biol 23(20): 7377-7390, 2003. DOI: 10.1128/MCB.23.20.7377-7390.2003

84 Ceci J, Patriotis C, Tsatsanis C, Makris A, Kovatch R, Swing D, Jenkins N, Tsichlis P, Copeland N: Tpl-2 is an oncogenic kinase that is activated by carboxy-terminal truncation. Genes Dev 11(6): 688-700, 1997. DOI: 10.1101/gad.11.6.688

85 Aoki M, Hamada F, Sugimoto T, Sumida S, Akiyama T, Toyoshima K: The human cot proto-oncogene encodes two protein serine/threonine kinases with different transforming activities by alternative initiation of translation. J Biol Chem 268(30): 22723-22732, 1993.

86 Roof D, Hayes A, Adamian M, Chishti A, Li T: Molecular characterization of abLIM, a novel actin-binding and double zinc finger protein. J Cell Biol 138(3): 575-588, 1997. DOI: 10.1083/jcb.138.3.575

87 Klimov E, Rud'ko O, Rakhmanaliev E, Sulimova G: Genomic organisation and tissue specific expression of ABLIM2 gene in human, mouse and rat. Biochim Biophys Acta 1730(1): 1-9, 2005. DOI: 10.1016/j.bbaexp.2005.05.001

88 Krupp M, Weinmann A, Galle PR, Teufel A: Actin binding LIM protein 3 (abLIM3). Int J Mol Med 17(1): 129-133, 2006.

89 Barrientos T, Frank D, Kuwahara K, Bezprozvannaya S, Pipes G, Bassel-Duby R, Richardson J, Katus H, Olson E, Frey N: Two novel members of the ABLIM protein family, ABLIM-2 and -3, associate with STARS and directly bind F-actin. J Biol Chem 282(11): 8393-8403, 2007. DOI: 10.1074/jbc.M607549200

*Received May 1, 2023*
*Revised May 22, 2023*
*Accepted June 15, 2023*